IEEE Access
Multidisciplinary ⋮ Rapid Review ⋮ Open Access Journal

Received 12 July 2022, accepted 5 September 2022, date of publication 8 September 2022, date of current version 19 September 2022.

Digital Object Identifier 10.1109/ACCESS.2022.3205312

RESEARCH ARTICLE

Improved Adaptive Protection Scheme Based Combined Centralized/Decentralized Communications for Power Systems Equipped With Distributed Generation

ALAA HMAM EL-HAMRAWY, AHMED ABDEL MORDI EBRAHIEM, AND ASHRAF IBRAHIM MEGAHED, (Member, IEEE)
Electrical Power and Machines Department, Alexandria University, Alexandria 5424041, Egypt
Corresponding author: Alaa Hmam El-Hamrawy (alaa.alhamrawy@alexu.edu.eg)

ABSTRACT Recently, numerical relays with communication capabilities have been employed to provide adaptive solutions for Distributed Generations (DGs) protection issues. This paper presents an adaptive protection scheme based on centralized and decentralized communication to address DG protection problems. The proposed method uses two directional relays in each feeder, one at the beginning (called forward relay) and one at the end (called reverse relay). These relays can communicate with each other and the central unit. The centralized communication occurs between the central unit and the relays in the system when any relay's status changes from connected to disconnected or vice versa. It aims to define the operation mode, islanding detection, and activate the relays settings to achieve proper coordination. Protective relays are coordinated using a Genetic Algorithm (GA) to optimize protection time. The optimization problem considers pick up current (Ipu), Time Multiplier Setting (TMS), Plug Setting Multiplier (PSM), and curve type. Decentralized communication, which occurs when any relay detects a fault, increases relays' accuracy and speed of decision-making. This paper also proposes a novel method for detecting High Impedance Faults (HIF), a significant difficulty for protecting engineers as it draws a very low current that conventional overcurrent relays fail to detect in most cases. HIF is detected using wavelet transform, symlet 8, detail 2 (d2), and relay communication. On the IEC benchmark microgrid, the suggested algorithm is tested. ETAP is used for load flow analysis and short circuit analysis, whereas MATLAB is used for GA optimization, HIF modelling, and wavelet transform routines.

INDEX TERMS Distributed generation, directional overcurrent relay, genetic algorithm, coordination time interval, time multiplier setting, plug setting multiplier, pickup current, wavelet transform.

I. INTRODUCTION

Insertion of Distributed Generation (DGs) has some drawbacks on stability, power quality, and protection of the system, depending on size, location, type, and number of DGs connected to the system, these drawbacks can limit both size and number of DGs connected to the system [1]. The addition of DGs increase the short circuit level and cause a current flow in a reverse direction, hence the connections of DGs into existing power systems cause loss of coordination, bi-directionality, and islanding operation.

The application of metaheuristic techniques proved to be an effective tool to solve the coordination problem as a nonlinear optimization problem. The objective function of such an optimization problem is to minimize the total operating time of all relays in the system regarding the constraints of the protection process. One of the most suitable metaheuristic techniques used to achieve proper

The associate editor coordinating the review of this manuscript and approving it for publication was Akshay Kumar Saha.

coordination amongst protective relays is Genetic Algorithm (GA) [2], [3], [4], [5], [6], [7], [8], [9], [10], [11], [12], [13], [14]. In [2], [3], and [4], the authors used the GA to calculate Time Multiplier Setting (TMS) as a decision variable for all relays in the system regarding the protection constraints. Following the same track, the authors in [5] made a comparison between GA and the dual simplex method to calculate TMS for relays. Also, in [6] it is proposed to use fuzzy-based GA to solve the optimization problem. In [7], [8], and [9] the authors applied the GA to calculate TMS and Pickup Current (Ipu) for each relay. It is noted that the previous mentioned researches [2], [3], [4], [5], [6], [7], [8], [9] used only one curve type in the protection process, thus the authors in [10] employed different types of curves to achieve the least time for the protection of the system. The algorithm was tested using only three types of curves. Additionally, the results showed that the algorithm chose only one curve type for most of relays in all modes of operations (islanding and grid connected modes). The Plug Setting Multiplier (PSM) has also been considered as a new constraint in [11]. In that work, the authors inserted the upper limit of PSM as a constraint in the optimization problem. Later on, the authors in [12] suggested using non-standard characteristics which are defined by a larger limit of PSM, where they assumed the upper value of PSM as 100. The authors proved the benefits of adding that constraint in the protection system, especially with the increased contribution of DGs to the network. The authors in [13] assumed the upper limit of PSM as a decision variable in the optimization problem which provided flexibility to the algorithm to find the best solution. Finally, the authors in [14] introduced a modification to the work presented in [13] by using different types of curves; where IEC and IEEE standard curves were used in the protection process. Based on that approach, three main decision variables have been used; namely TMS, upper limit of PSM, and curve type.

Islanding operation has some drawbacks on the system such as voltage and frequency control, power quality, lack of grounding, and out-of-phase reconnection [15]. Islanding detection techniques are categorized in two essential groups; local techniques and remote (communication based) techniques. The local techniques are divided into passive, active, and hybrid techniques. The local detection techniques are based on measuring system variables, such as voltage, frequency, active power, reactive power, at DG location [17], [18], [19], [20], [21], [22]. Although these techniques have low cost, they give poor results in some cases, especially when a matching between load and DG occurs during islanding operation, resulting into a large non-detection zone [16]. Communication based techniques use a continuous signal between grid and DGs and are classified into power line signaling scheme and transfer trip scheme, where both schemes have an enhanced reliability compared to the local techniques, however, with a higher cost.

The presence of HIF without detection and isolation represents a significant danger on one's safety and may cause fires due to the existence of electric arc. One of the effective tools to detect the HIF is the expert system which depends on using artificial intelligence. This technique gives accurate results, but it needs a lot of time to detect the fault. While the authors in [23] used artificial intelligence to detect HIF, the authors in [24] make comparison between methods used fuzzy logic algorithm to detect HIF, and the authors in [25] used the nonlinear voltage–current characteristic. Some authors suggested using a combination of fuzzy logic and genetic algorithm [26]. Amongst the most popular techniques, wavelet transform is used to detect HIF. The ability of wavelet transform to decompose a signal into different frequency bands and location in time, with various types of wavelet mother function, can be used to detect HIF [27], [28], [29].

An adaptive protection can be implemented either in a centralized manner by using a microgrid central controller to change the active-group settings [30] or in a decentralized manner in which the relays in the microgrid change their own active-settings groups by receiving a trip-signal/breaker status from another relay or circuit breaker. Previously, the adaptive protection for the AC microgrid using centralized protection and communication architecture was proposed in [30], [31], and [32]. An adaptive overcurrent protection for microgrids using inverse-time directional overcurrent relays (DOCRs) was presented in [33]. An adaptive protection combined with machine learning for medium voltage microgrids was reported in [34]. A new adaptive protection coordination scheme based on the Kohonen map or self-organizing map (SOM) clustering algorithm was proposed recently in [35] for the inverse-time OC relays. A decentralized adaptive protection scheme using DOCRs, tele protection and a fuzzy system in real time was proposed in [36] for the transmission system. An optimal overcurrent relay coordination in the presence of inverter-based wind farms and electrical energy storage devices was presented in [37]. An adaptive protection system based on the IEC 61850 for MV smart grids was presented in [38]. A detailed survey of different adaptive protections of microgrids was presented recently in [39]. For a further detailed review of different microgrid protection schemes, their challenges and developments, the recent review articles [40], [41], [42], [43] are suggested.

The previous review shows that many efforts are oriented toward solving the protection problems associated with the connection of DGs. However, each method focuses on solving only one problem, and there is no method that solves all problems. Also, all the adaptive and communication-based methods do not provide HIF classification and detection [42].

In this paper, the suggested method addresses all protection issues originating from the connection of DGs, including loss of coordination, bi-directionality, and islanding detection. In addition, the proposed algorithm provides a detection method for HIF, which is prevalent in medium voltage networks and presents a significant challenge to protection engineers due to the fact that it draws a very low current that conventional overcurrent relays, in most cases, fail to detect. The algorithm employs two directional and numerical

relays with communication capabilities at each end of each feeder. A combination of centralized and decentralized communication is utilized to boost the protection system's precision and speed, as well as to decrease the amount of data carried over the communication link in order to solve the issue of data loss and delay. When any relay in the system changes its status from connected to disconnected or vice versa, centralized communication is established between all relays and the central unit. This communication is intended to identify the operation mode (OM), detect islanding, and activate the relay settings in order to achieve proper coordination between them. Using the Genetic Algorithm (GA) as an optimization technique, protective relays are coordinated to ensure the shortest possible protection time. In the optimization problem, all relay variables, including Ipu, TMS, PSM, and curve type, are evaluated. Despite the fact that decentralized communication reflects the communication between the relays in each feeder and that it occurs when any relay detects a fault, this communication tends to improve the precision and speed of relay decisions. In addition, Wavelet transform, symlet 8, detail 2 (d2), and decentralized communication between relays are employed to identify and isolate the HIF.

The paper contributions are:

1- All relay variables, including Ipu, TMS, PSM, and curve type, are considered in the optimization problem when using GA as an optimization tool to solve a loss of coordination problem. All previous studies have only considered one or a subset of the variables in the optimization problem [2], [3], [4], [5], [6], [7], [8], [9], [10], [11], [12], [13], [14]. This reduces the protection time for relay coordination in each OM.

2- A novel HIF detection technique based on wavelet transform. Symlet 8 is used as the mother wavelet function, and detail 2 is used to extract signal features that differentiate HIF from other events. For fault detection, the sum of the square values of d2 throughout a single cycle is determined. Through decentralized communication, a choice is made based on the detection of HIF from both relays on the same feeder. All previous work depended on the detection of HIF from a single relay, which in some cases resulted in false tripping or prolonged the detection time [27], [28], [29].

3- Proposing a system protection algorithm based on a hybrid of centralized and decentralized communication between relays. All previous research employs either centralized or decentralized communication between relays to solve a system problem. In the proposed algorithm, centralized communication between a central unit and the system's relays identifies the system's OM and defines the relays' settings. While the decentralized communication between relays on the same feeder allows for a quick and accurate trip decision, this communication also allows for the relays to operate independently. The proposed combination reduces relay data transfer complexity. Additionally, this combination improves the protection system's decision-making precision and speed.

4- The proposed algorithm provides a solution for all protection issues resulting from the connection of DGs, as well as the detection of HIF. According to the author of [42], the majority of adaptive solutions do not provide detection and classification of HIF.

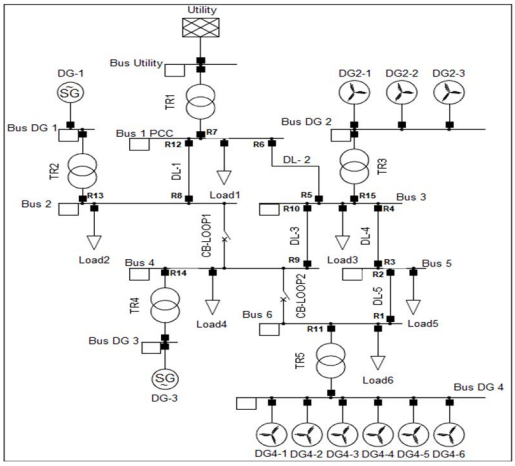

FIGURE 1. IEC benchmark microgrid.

II. SIMULATION OF THE TESTED SYSTEM

The simulated system in this study is IEC benchmark microgrid shown in Fig. 1. The system parameters are presented in [44]. This system consists of utility and four DGs connected at different buses and different ratings as shown in the figure. There are five main feeders in the system; DL-1 to DL-5, switches SW1 and SW2, which are considered open in this study, and the base voltage is taken as 25 kV. The simulation of the system and the required studies are performed using MATLAB and ETAP programs.

The system depicts four main operating modes, the first is operating mode 1 (OM 1), where only the main grid is connected and all DGs are disconnected. This operating mode represents the old version of electrical system with radial configuration. The second is operating mode 2 (OM 2), in which all sources in the network are connected, which means the utility and all DGs are in service. Consequently, this operating mode represents the complex configuration of the protection system since the current will flow in both directions and the short circuit level will increase due to the contribution of the connected DGs. In operating mode 3 (OM3), only the utility DG1, and DG2 are connected whereas DG3 and DG4 are disconnected. This case represents a case of partial contribution of DGs that ranges between the maximum contribution (OM 2) and the zero contribution (OM 1). Operating mode 4 (OM 4) is the islanding mode where all DGs are connected and the utility itself is out of service. The operating modes of the tested system are summarized in table 1.

TABLE 1. Operating modes of IEC benchmark microgrid.

Operating mode	Utility	DG1	DG2	DG3	DG4
OM 1	In service	Out of service	Out of service	Out of service	Out of service
OM 2	In service	In service	In service	In service	In service
OM 3	In service	In service	In service	Out of service	Out of service
OM 4	Out of service	In service	In service	In service	In service

III. PROPOSED ALGORITHM

The proposed method depends on using two directional relays in each feeder to isolate the feeder from both sides because of the connection of DGs (one of them at the beginning of the feeder and called forward relay and the other one at the end of the feeder and called reverse relay). Each relay has the ability to communicate with the central unit (centralized communication) and with the relay in the same feeder (decentralized communication). With the notions of smart grids and microgrids, this configuration becomes accessible and familiar in current networks.

The IEC 61850 communication standard is the proposed communication standard in this work. Due to the promise of interoperability between Intelligent Electronic Devices (IEDs) from different manufacturers, its use in the automation of electric power substations has increased dramatically. As a common protocol, the IEC 61850 standard enables the integration of all protection, control, measurement, and monitoring functions [45].

The IEC 61850 communication architecture has three levels: process level, bay level, and substation level. At the process level, Merging Units (MUs) will collect and digitize the electrical parameters measurement data (MMXU) from the voltage and current sensors and status of the circuit breakers (XCBR) within the grid. IEDs for lines and DGs will collect digitized measurement data (MMXU) and circuit breaker status signals (XCBR) from the process bus at the bay level. Each MU will publish data to the process bus, while each IED will subscribe to the respective published data. In the event of faults, each line and DG IED will use measurement data (MMXU) from their respective MU to perform active protection functions such as overcurrent protection [45].

The suggested protection algorithm consists of offline calculations executed prior to system operation and online calculations and communications executed while the system is in operation, as illustrated in Fig. 2.

A. OFFLINE CALCULATIONS TO SOLVE LOSS OF COORDINATION PROBLEM

This part tends to perform offline calculations to determine relays settings for each OM; these settings ensure speedy and accurate coordination.

In this paper, GA is used to coordinate DOCRs under various OMs. In the optimization problem, three main variables

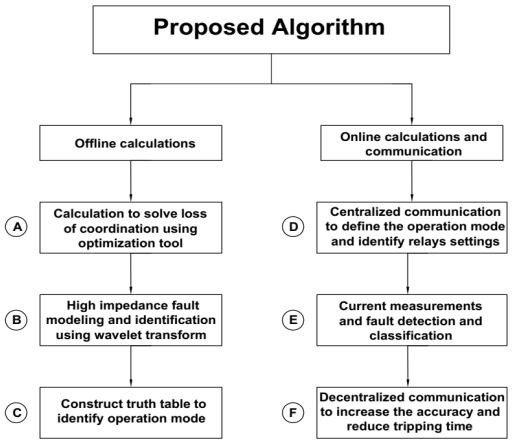

FIGURE 2. Outlines of the proposed algorithm.

are considered as decision variables for each relay in the system. These variables are Ipu, TMS, and the type of curve, which includes all IEC and IEEE standard curves. In addition, the PSM can be assigned any value without limitations, as considered by the nonstandard characteristic curve for relays. Simulation of the system, load flow analysis, and short circuit calculations are all performed with ETAP program and are used as inputs to the GA routine, whereas the optimization problem using GA can be constructed with MATLAB Optimization Toolbox.

The objective function is to minimize the total operation time of all protective relays in the system as indicated in (1). Knowing that, n is the number of faults, m is the number of relays, and t_p and t_s are the operating time of the primary and backup relays respectively.

$$Min \sum_{i=1}^{m} \sum_{f=1}^{n} (t_p + t_s) \tag{1}$$

The operating time for relays can be calculated from the standard equation described in (2).

$$t_i = \frac{A * TMSi}{(\frac{I_{fi}}{I_{pui}})^B} + C \tag{2}$$

where TMS_i is the time multiplier setting of relay i, I_{fi} is fault current, I_{pui} is the pickup current of the relay i, I_{fi} /I_{pui} is Plug Setting Multiplier (PSM) of relay i, and A, B, and C are constants that define the relay characteristic curve as shown in table 2 [14].

The main variables and constraints for the optimization problem are:

- The Coordination Time Interval (CTI) which represents the time margin between the primary and back up relay as described in (3). The most common used value of CTI is between 0.2 and 0.5 sec. In this work, CTI is set as 0.2 sec.

$$t_{si} - -t_{pj} \geq CTI, i, \quad j = 1, 2, 3, \ldots\ldots m \tag{3}$$

- For each relay, the lower and upper limits of TMS, taken as 0.025 and 1.02 respectively, are included as in (4).

$$TMS_{i\,min} \leq TMSi \leq TMSi_{max} \tag{4}$$

TABLE 2. Defining curve type and curve parameters in the optimization problem.

Curve no.	Curve name	A	B	C
1	IEC Short Time Inverse (STI)	0.05	0.04	---
2	IEC Standard Inverse (SI)	0.14	0.02	---
3	IEC Very Inverse (VI)	13.5	1	---
4	IEC Extremely Inverse (EI)	80	2	---
5	IEC Long Time Inverse (LTI)	120	1	---
6	IEEE Moderately Inverse (MI)	0.0515	0.02	0.114
7	IEEE Very Inverse (VI)	19.61	2	0.491
8	IEEE Extremely Inverse (EI)	28.2	2	0.1217
9	IEEE Inverse (I)	44.6705	2.0938	0.8983
10	IEEE Short Inverse (SI)	1.3315	1.2969	0.16965
11	IEEE Long Inverse (LI)	28.0715	1	10.9296

- The pickup current should be bounded such that it must be larger than the maximum load current and lower than the minimum fault current as indicated in (5).

$$I_{i\,pickup\ min} \leq I_{i\,pickup} \leq I_{i\,pickup\,max} \tag{5}$$

- If standard characteristics are adopted, then, the PSM is ranging between 5- 20. However, the authors in [12], [13], and [14] suggested non-standard characteristics where PSM can generally take any value with no restriction (6). Thus, the PSM will not be considered in the optimization problem but it will be treated as a dependent variable. Its value will be calculated after the optimization problem returns the value of pickup current and by knowing the value of the maximum short circuit current for each relay. Therefore, constraint (6) will hold.

$$PSM_i \epsilon non - standard\ characteristics\ value \tag{6}$$

- The characteristic curve type is determined by the values of *A, B,* and *C* as described in table 2. In this work, the curve type is defined as an integer in the optimization problem. Similar to a lookup table, a simple function is then used to define the curve type, as shown in (7). Each curve is described by an integer variable in the optimization problem (from 1 to 11 as shown in first column in table 2).

$$CS \epsilon Standard\ curves \tag{7}$$

For comparison purpose, this paper proposes a proper and effective optimal relay coordination algorithm for distribution system equipped with DGs. In the optimization problem, all relay parameters are taken into account as decision variables, whereas only a subset of relay parameters were taken into account in previous work, as discussed in the literature. Table 3 compares the contribution of the current work to that of previously presented work in terms of the consideration

TABLE 3. Contributions of the present work compared with the previous work.

Paper	I_{pu}	TMS	PSM	CS
Paper [2-6]	No	Yes	No	No
Paper [7-9]	Yes	Yes	No	No
Paper [10]	Yes	Yes	Standard	IEC standard curves
Paper [12]	No	Yes	Constant, non-standard	No
Paper [13]	No	Yes	Variable, non-standard	No
Paper [14]	No	Yes	Variable, non-standard	IEC and IEEE standard curves
Present work	Yes	Yes	Variable, non-standard	IEC and IEEE standard curves

(Yes) and non-consideration (No) of different variables and constraints.

B. OFFLINE CALCULATIONS TO MODEL AND CHOOSE METHOD TO DETECT HIF

The offline calculations of a novel method for detecting the HIF are presented in this section. The criteria must go through HIF modelling before employing a method to detect it.

1) MODELING OF HI

Several models have been proposed in the past to represent HIF, such as modelling the fault as a fixed resistance. Nonlinear resistance was employed to modify this model. Additionally, the use of two anti-parallel diodes coupled to a DC source has been proposed. As a modification, one or two fixed or variable resistances are added to this model. Other strategies used transient analysis of control systems (TACS) to control the fault's connection and resistance value [27], [28], [29].

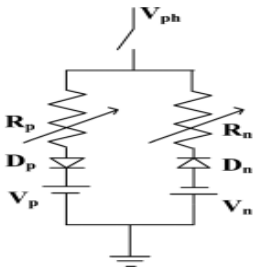

FIGURE 3. Model of HIF.

The HIF model used in this paper is described in [46] and illustrated in Fig. 3. The model is comprised of two anti-parallel diodes linked to various dc sources and variable resistances. The value of Vp is 6 kV with a random variation of ±10%, while the value of Vn is 3 kV with a random variation of ±10%. The values of variable resistances vary arbitrarily between 600 and 900 Ohm. Every 0.1 ms, the values of sources voltages and resistances are altered.

The model parameter values must be adjusted so that the HIF current value is less than 10% of the normal current in the system being tested.

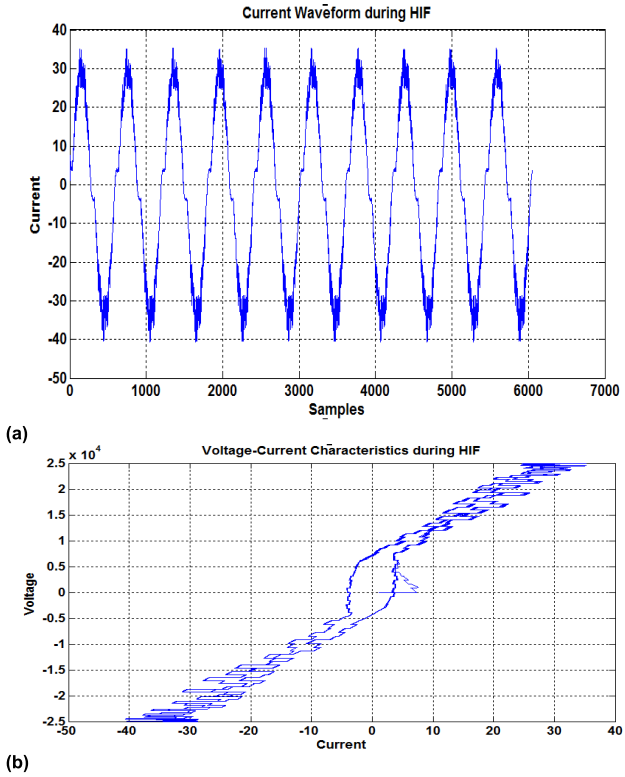

FIGURE 4. (a) Current wave during HIF, (b) V-I characteristics of HIF.

The HIF model is implemented using Matlab-Simulink. The variable DC sources are modelled with controlled voltage sources that change randomly every 0.1 ms, whilst the variable resistances are modelled with 20 parallel resistances of varying values that are switched between every 0.1 ms. Fig. 4 (a) depicts the current wave during HIF, whereas Fig. 4(b) demonstrates the V-I features of HIF. The retrieved current waveform and voltage-current characteristics during HIF are similar to those described in [27] and [46].

2) HIF DETECTION USING WAVELET TRANSFOR

Wavelet Transform (WT) is utilized in a multitude of applications, including signal analysis and signal processing. Using WT, a signal is decomposed into multiple frequency bands. The mother wavelet is a zero-mean-valued predefined function that is used to compress or decompress and shift in time. Using wavelet, time-frequency data can be provided. By importing the signal through high pass and low pass filters, two coefficients referred to as detail and approximation are produced [47]. Repeating the procedure on the output of the low pass filter (approximately) will yield two new coefficients, and so on.

The output of the wavelet transform is utilized to determine a variety of power system conditions. To detect the HIF, many researchers have utilized the wavelet transform for this reason. This paper will utilize it as well, but with a new technique that reduces the time required to detect the fault and improves its accuracy compared to previous works.

The proposed method uses wavelet transform and communication relays located at the beginning and end of each feeder in the system. Through several tests using different wavelet mother functions and details, it is observed that symlet 8 as the wavelet mother function and detail 2 as the level of decomposition (d2) is provide best features for distinguishing HIF from other events. The value of d2 fluctuates between negative and positive values with a large difference between the HIF condition and other events; therefore, the fault will be identified by calculating the sum of the squares of the values of d2 over a single cycle (K), as in (9).

$$K = \sum_{\text{over one cycle}} (\text{Values of d2}) \wedge 2 \tag{8}$$

To maximize the difference between the value of the K factor under normal conditions and fault conditions, the square of the values of d2 is calculated. This criterion has demonstrated its ability to accurately detect the HIF. On both sides of each feeder, this criterion will be applied to the current signal. The calculated values (K_f at the forward relay and K_r at the reverse relay) are subsequently compared to a threshold value. There is a significant difference between the calculated values of K_f and K_r under HIF conditions and those under other conditions. Therefore, it is very simple to select the threshold value for any system, given that the decision will be based on two different values from two relays in two different locations. This criterion achieves superior performance (high accuracy and speed) in detecting HIF compared to other researches, which take longer to detect the fault and, in some cases, cause false trips due to their reliance on only one side to detect the fault. In the results section, the effectiveness of the proposed method will be demonstrated by comparing it to the results extracted from other papers.

C. CONSTRUCT A TRUTH TABLE TO IDENTIFY THE OM

This section tends to construct a truth table that will be used by the central unit to identify the OM. The constructed truth table is shown in table 4 and is based on the configuration and the defined OMs of the tested system, as shown in Fig. 1 and table 1 respectively. The status of the relays is defined by a mark (0), (1), or (×) in the truth table, where the mark (1) indicates that the relay is connected, the mark (0) indicates that the relay is disconnected, and the mark (×) indicates that the status of the relay will not affect defining the OM (in digital circuits, this situation is referred to as ''do not care'').

As shown in table 1, OM 1 is defined by the connection of only the utility and the disconnection of all DGs. Consequently, based on the configuration of the tested system depicted in Fig. 1, the central unit must receive a signal from R7, the utility side relay, indicating that it is in service. In addition, the central unit must receive an out-of-service signal from all relays at DGs, which are R11, R13, R14, and R15. It is important to note that the status of the reset relays

TABLE 4. Truth table to identify the OM of the system.

Relay	OM 1	OM 2	OM 3	OM 4
R1	×	1	×	1
R2	×	1	×	1
R3	×	1	×	1
R4	×	1	×	1
R5	×	1	1	1
R6	×	1	1	1
R7	1	1	1	0
R8	×	1	1	1
R9	×	1	×	1
R10	×	1	×	1
R11	0	1	0	1
R12	×	1	1	1
R13	0	1	1	1
R14	0	1	0	1
R15	0	1	1	1

of the feeders will not have affected the identification of this OM. For example, the connection or disconnection of R6 or R5 or R4 or any other feeder relay will not change the OM if all DGs are disconnected. This is the reason why the status of the feeders relays are marked with 'do not care' status in the truth table to define OM 1.

For OM 2 to be defined, the central unit must receive a connection signal from the utility relay and all DG relays indicating that they are all in service. Additionally, in this OM, all feeder relays must be connected. If R5 or R6 or any other feeder relay is disconnected, for instance, this indicates that the sources are not connected, which is not defined as OM2. Therefore, the status of all feeder relays is considered when defining OM 2. The same criteria are used to define OM 3 and OM 4

In contrast, the online calculations are performed during the system is in operation and they are:

D. CENTRAL COMMUNICATION BETWEEN CENTRAL UNIT AND RELAYS

In this section, communication is established between the central unit and all relays in the system to define the OM and activate the appropriate relay settings for each OM, based on offline calculations performed prior to system operation.

This signal describes the status of the relay (connected/disconnected) and will be transmitted to the central unit by all system relays. The central unit uses the signal from the relays to determine the mode of operation of the system using the truth table in table 4 that was constructed early on. Using AND and NOT gates, the truth table can be converted into a simple digital circuit. The central unit then transmits a signal to all system relays, informing them of the current OM. In accordance with offline calculations, the relays will activate the appropriate settings for the OM.

Notably, if the status (connected/disconnected) of any relay in the system changes, it will send a signal to the central unit containing the new status. The central unit will then send a signal to each relay to activate the appropriate settings for the new OM. This communication will only take 40 ms (20 ms for the signal from relay to the central unit and 20 ms for the signal from central unit to all relays in the system [45]). In addition, this communication will have occurred only if the status of any relay in the system has changed. In most instances, the time required to identify the OM will not impact the time required to isolate a fault by relay.

E. FAULT DETECTION AND IDENTIFICATION

This section is executed in online mode and is designed to identify and detect overload, short circuit, and high impedance faults.

The offline calculations using GA were performed and present a solution for overload and short circuit faults detection. By applying the optimization problem and calculating the settings for each relay in all OM, the relay is able to identify overload and short circuit faults by comparing the measured current value to the pickup current, thereby calculating the tripping time based on its predefined characteristic curve.

In addition, offline calculations were performed for the HIF, presenting a novel method for detecting faults of this type. Using wavelet transform, symlet 8 was used as the mother wavelet function, and the sum of the square of the values of detail 2 over one cycle (20 ms) was employed to identify the fault. The relay will therefore apply this criterion to the measured current in order to identify the HIF.

F. DECENTRALIZED COMMUNICATION BETWEEN RELAYS

Now is the time to emphasize the significance of decentralized relay-to-relay communication. Communication is decentralized only between the two relays on the same feeder. This communication can be used to decrease the required time for the protection system and to enhance the protection process in certain circumstances.

The concept is to use decentralized communication between each pair of relays, so that when each relay detects a fault, they will communicate with one another. According to this communication, the relays will trip even if the trip time for each of them has not been reached. Consequently, this will decrease the necessary protection time for the two relays. In addition, there is no requirement for central communication in this instance, allowing for simple implementation, reduced communication time, a dependable connection, and no data loss.

In order to be more specific and to demonstrate the effectiveness of decentralized communication, in OM 2, R4's operation time is 0.2081 s and R3's operation time is 0.9537 s without any communication between them as extracted from the results section. However, if the two relays communicate with one another and both trip if a fault is detected, the trip time for both relays will be shortened, as required by the protection process. The trip time with communications will be the sum of the fault detection time and the relay-to-relay communication time. The communication time between relays in the same feeder will not exceed 20 ms [45]. The detection time is only one cycle, or 20 ms, which is required

to measure current. Therefore, the required time to trip each relay is less than 50 ms when relay delay is taken into account.

In the event of a communication failure, each relay will trip according to its characteristic curve after a tripping time. This is acceptable for the protection process, but it will negate the time-saving effect of the communication link.

IV. RELAY PROGRAMMING AND OPERATION

A flowchart for R4 will be used as an example for forward relays to explain the operation of the entire relay program. In addition, a flowchart for R3 will be described as an illustration for the reverse relays. It is important to note that the forward and reverse relays utilize the same flowchart with minor modifications, as depicted in the following section.

Fig. 5 depicts the programming of the forward relays; the relay operation can be described by tracing the flowchart as follows:

- When the OM changes, the relay begins by receiving a signal from the central unit via centralized communication. The received signal specifies the new OM to the relay; consequently, the relay will activate the correct settings to achieve correct coordination between relays based on the results of the optimization problem performed using GA.

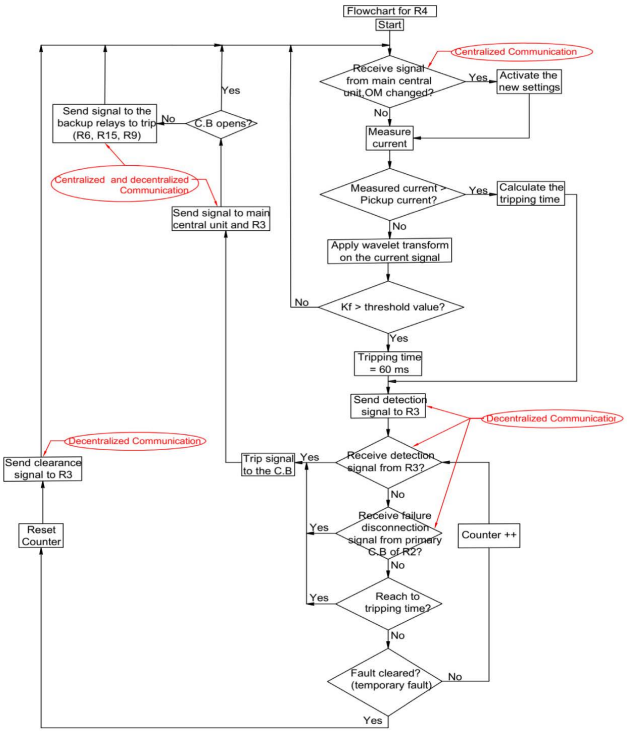

FIGURE 5. Flowchart for the forward relays, R4 as example.

- The relay will then compare the measured current to the pickup current to protect the system from overload and short circuit faults. If the relay detects a fault, it will determine the tripping time based on its characteristic curve and the measured current value. Only if the decentralized communication between relays in the same feeder is lost will the relay trip after this tripping time. However, due to the presence of communication between relays, the isolation time will be less than the time calculated from the characteristic curve of the relay. The isolation time is the sum of the time required for current measurement and fault identification (20 ms), decentralized communication between relays (20 ms), and circuit breaker operation (20 ms) [45].
- If the measured current indicates normal operation, the relay will analyze the current waveform using wavelet transform, symlet 8 mother wavelet function, and the sum of details 2 over one cycle will be computed as previously described. This analysis tends to recognize HIF if it exists. In this study, the tripping time is set at 60 ms (time for relay to verify fault detection) if the relay detects HIF. This time provides rapid isolation of the faulty feeder in the event of a loss of communication between relays on the same feeder. Additionally, this delay guarantees distinction between the HIF and other conditions such as load switching and capacitor switching to avoid false tripping. With the existence of communication between relays, however, the isolation time is the same as calculated in the previous paragraph: the sum of the time required to measure the current and fault identification (20 ms), the time required for decentralized communication between relays (20 ms), and the time required to operate the circuit breaker (20 ms) [45].
- After the relay detects the fault, it will send a signal to the relay in the same feeder via decentralized communication. In addition, the relay will check if it has received a signal from the relay in the same feeder indicating that it, as well, has detected a fault. If the relay receives this signal, it will trip immediately without waiting for the tripping time as the fault detection is checked by both relays.
- Additionally, using decentralized communications between relays, the operation of the relay as a backup relay can be modified. If the relay receives a signal from the relay in other feeders describing the disconnection failure of the circuit breaker for which the relay is a backup, it will trip immediately without waiting for the tripping time, as the fault detection is checked by the primary relay and the breaker fails to disconnect the circuit. If the relay does not receive the signal from other relays, it will continue counting until the tripping time is reached, at which point it will trip.
- When the relay trips as the primary or backup relay for any type of faults, it sends a signal to the central unit and the relay in the same feeder. If the relay detects fault clearance (temporary fault), it will reset the counter and send a status signal to the relay in the same feeder.
- For permanent faults, the relay will check for the breaker's disconnection; if the breaker fails to

disconnect the circuit, the relay will signal all backup relays to immediately disconnect the circuit.

- It is worth noting that in the event of a communication failure between relays, the relay will continue to protect the system against a variety of fault types in a fast and accurate manner. The tripping time required to protect the system against overloads and short circuit faults is calculated based on the characteristic curve of the relay, which is defined using offline GA calculations. In addition, the required trip time to protect the system against HIF is 60 ms, which is also a fast trip time. However, if communication is lost, each relay will operate independently, and the system will lose the benefit of isolating the faulty section based on fault detection on both sides.

In contrast, with minor modifications, the operation of R3 as a reverse relay is identical to that of R4 as a forward relay. It is essential to note that R3 and R4 are in the same feeder. In some OMs, the reverse relays do not detect any current at the beginning of the program because there is no connected supply behind the relay. For instance, all reverse relays in OM 1 will have no settings because all DGs are out of service and there is no other source of power in the network besides the utility. In the case of R3, there is no current passes through the relay in OM 1 and OM 3. In OM 3, only DG 1 and DG 2 are in service, while DG 3 and DG 4 are out of service. Therefore, no current will flow through the relay in this OM. This is why the relay should begin by determining whether the current OM is OM 1 or OM 3. If the response is negative, the relay will continue as per R4. If the answer is yes, the relay will only trip if it receives a trip signal from R4, which is located in the same feeder, in order to completely isolate the feeder under fault conditions.

V. RESULTS

A. RESULTS OF OFFLINE CALCULATIONS TO SOLVE LOSS OF COORDINATION

Recall that the proposed algorithm considers all quantities in the relay equation - Ipu, TMS, PSM, and CS - as variables; three of them, Ipu, TMS, and CS, are decision variables in the optimization problem, while PSM is a dependent variable.

The load flow analysis will be performed for each OM and used as an input to the GA to determine the pickup current for each relay in the system. In addition, the short circuit current at each bus will be calculated and used to determine the PSM for each relay. GA will use the input data and constraints (The constraints are divided into lower limits, upper limits, and CTI between primary and back up relays as shown in equations (1)- (7)) to determine the parameters for each relay, and the results will be displayed in a table containing TMS, Pickup current, PSM, curve type, and operation time for each relay as primary protection. Given that the fault location is at the beginning of the feeder, another table will display the operating time for primary and backup relays for each feeder.

1) RESULTS FOR OM 1

In OM 1, all DGs are out of service and only the utility is connected. This mode represents the network's radial structure. Therefore, only the forward relays are considered in the optimization problem, only the forward relays are to be coordinated using GA.

Table 5 shows the results of all variables for all relays when the proposed algorithm is applied. The table demonstrates that all constraints are satisfied within the acceptable margin. Moreover, according to the non-standard curve utilized in this study, the value of PSM is free to vary. Table 6 displays the operating time of primary and backup relays for all fault locations, demonstrating that the CTI between relays has been attained.

TABLE 5. Relays characteristics for OM 1.

Relay	TMS	Pickup current (A)	PSM	Curve type	Operating time (sec)
R2	0.6827	208.30	40.56	IEC Extremely Inverse (EI)	0.0332
R4	1.1217	435.26	20.51	IEC Extremely Inverse (EI)	0.2137
R6	0.3249	926.18	10.22	IEEE Moderately Inverse (MI)	0.4587
R7	0.6028	1290	7.34	IEEE Very Inverse (VI)	0.7145
R10	0.0407	220.24	40.54	IEC Extremely Inverse (EI)	0.0020
R12	0.4198	252.63	37.48	IEEE Very Inverse (VI)	0.4969

TABLE 6. Operating time for primary and backup relays.

Fault location	Operating time of primary relay (sec)		Operating time of backup relays (sec)		CTI between primary and backup relays (sec)	
DL-1	R12	0.4969	R7	0.7145	R7-R12	0.2176
DL-2	R6	0.4587	R7	0.7145	R7-R6	0.2557
DL-3	R10	0.0020	R6	0.4679	R6-R10	0.4659
DL-4	R4	0.2137	R6	0.4679	R6-R4	0.2542
DL-5	R2	0.0332	R4	0.2387	R4-R2	0.2055

Table 7 compares the total operation time of the primary and backup relays between the present work and some previous work. This paper demonstrates that the total protection time achieved is shorter than in previous research. The reason why the total time achieved in [11] , [12], and [13] is greater than that achieved in [14] and the current work is because those papers solved the optimization problem using a single curve type as opposed to multiple curve types.

2) RESULTS FOR OM 2

The utility and all DGs are connected in this OM. Consequently, the current may flow in both directions, and the

TABLE 7. Comparison between total operating time in previous and present work.

Work	Paper [11]	Paper [12]	Paper [13]	Paper [14]	Present work
Total operating time (s)	7.53	6.64	4.99	3.86	3.34

short circuit level will increase as a result of the connected DGs. In light of this, every relay will be considered in the optimization problem.

Table 8 shows the results of all variables for all relays when the proposed algorithm is applied. Table 9 shows the operation time for both primary and backup relays at each fault location. The tables demonstrate that all constraints are satisfied within an acceptable range.

TABLE 8. Relays characteristics for OM 2.

Relay	TMS	Pickup current (A)	PSM	Curve type	Operating time (sec)
R1	1.1085	170.06	8.05	IEC Extremely Inverse (EI)	1.3879
R2	0.1202	140.62	75.09	IEC Extremely Inverse (EI)	0.0017
R3	0.8567	59.43	22.71	IEEE Inverse (I)	0.9537
R4	0.1459	261.63	43.34	IEEE Moderately Inverse (MI)	0.2081
R5	0.6563	7.04	418.5	IEC Standard Inverse (SI)	0.7161
R6	0.9291	426.21	24.33	IEEE Very Inverse (VI)	0.5218
R7	0.6685	724.73	13.06	IEEE Moderately Inverse (MI)	0.7540
R8	0.5818	19.53	46.33	IEEE Inverse (I)	0.9067
R9	0.6999	11.92	75.89	IEC Long Time Inverse (LTI)	1.1214
R10	0.0543	277.72	42.41	IEEE Extremely Inverse (EI)	0.1226
R11	0.5865	232.44	3.89	IEEE Moderately Inverse (MI)	1.1887
R12	0.1683	370.76	33.33	IEEE Very Inverse (VI)	0.4940
R13	0.8780	339.73	4.03	IEEE Very Inverse (VI)	1.6192
R14	0.6551	238.54	3.79	IEEE Moderately Inverse (MI)	1.3381
R15	0.4282	163.34	4.35	IEEE Very Inverse (VI)	0.9589

OM 3 and OM 4 undergo the identical procedure. Therefore, each relay has four distinct settings, one for each OM, and these settings ensure proper coordination between relays.

B. RESULTS OF OFFLINE CALCULATIONS TO DETECT HIF

The proposed method is applied to feeder DL-4 that is equipped with R3 and R4 in the different cases as follow:

1) NORMAL CAS

Fig. 6 depicts the change in K_f at forward relay R4, which is the sum of the squared values of d2 over one cycle. This number indicates that the value of K_f is close to zero.

TABLE 9. Operating time for primary and backup relays.

Fault location	Operating time of primary relay (sec)	Operating time of backup relays (sec)			CTI between primary and backup relays (sec)		
DL-1	R12 0.4940	R7 0.7540	R5 0.7186		R7-R12 0.2600	R5-R12 0.2246	
	R8 0.9067	R11 1.1887			R11-R8 0.282		
DL-2	R6 0.5218	R7 0.7540	R8 0.9069		R7-R6 0.2322	R8-R6 0.3851	
	R5 0.7161	R15 0.9589	R3 0.9546	R9 1.1290	R15-R5 0.2428	R3-R5 0.2385	R9-R5 0.4129
DL-3	R10 0.1226	R6 0.5260	R15 0.9589	R3 0.9546	R6-R10 0.4035	R15-R10 0.8363	R3-R10 0.832
	R9 1.1214	R14 1.3381			R14-R9 0.2167		
DL-4	R4 0.2081	R6 0.5260	R15 0.9589	R9 1.1290	R6-R4 0.3179	R15-R4 0.7508	R9-R4 0.9209
	R3 0.9537	R1 1.4300			R1-R3 0.4763		
DL-5	R2 0.0017	R4 0.2100			R4-R2 0.2083		
	R1 1.3879	R13 1.6192			R13-R1 0.2313		

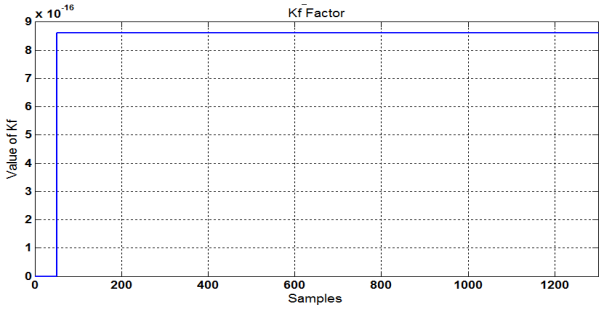

FIGURE 6. The value of Kf at forward relay.

On the other hand, Fig. 7 depicts the change in the value of K_r at reverse relay R3, which is the sum of the squared values

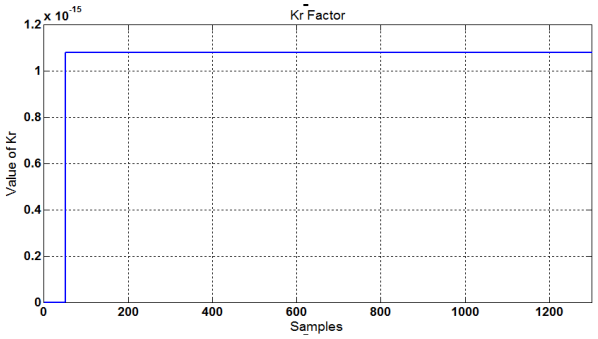

FIGURE 7. The value of Kr at reverse relay.

of d2 over one cycle. This number indicates that the value of K_r is close to zero.

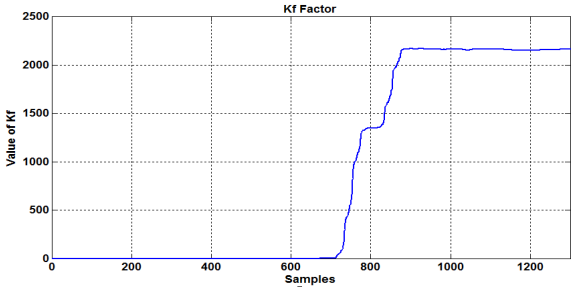

FIGURE 8. The value of Kf at forward relay.

2) HIF AT A DISTANCE OF 50% OF THE LINE

The fault was introduced at 0.09 s. Fig. 8 shows the change in K_f. The graph demonstrates that the value of K_f during fault is always greater than 2000.

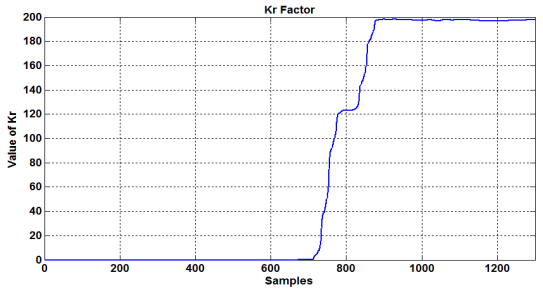

FIGURE 9. The value of Kr at reverse relay.

Fig. 9 shows the change in the value of K_r at reverse relay R3. This number indicates that the value of K_r is close to 200.

The identical procedure was repeated for various cases and fault locations. Table 10 summarizes all case results. Nonetheless, there is a significant value disparity between the fault cases and the other cases. Both relays will make the tripping decision so that it will be more accurate and prevent the making of an incorrect decision.

In certain cases (case 6: capacitor switching on the reverse relay side), the value of K_r is greater than the value of K_r in some fault condition (case 3), indicating that an incorrect decision may be made. This is correct if the decision was dependent on only one relay (as in previous work), but in this study, the decision will be made from both sides, eliminating the possibility of making a wrong decision. In addition, switching (loads or capacitors) occurs in a small number of samples, but the decision is made if the values of K_f and K_r exceed the threshold value for a cycle (20 ms).

TABLE 10. Results of the value of Kf and Kr for all cases.

case	Sum of square values of d2 over cycle for current at forward relay (K_f)	Sum of square values of d2 over cycle for current at reverse relay (K_r)
Case 1: normal case	0	0
Case 2: HIF at middle of the line	>2000	200
Case 3: HIF at 10% of the line	>3000	~8
Case 4: HIF at 90% of the line	>1200	>600
Case 5: load switching	~1	~1
Case 6: capacitor switching at reverse relay side	~33	~33
Case 7: capacitor switching at forward relay side	0	0

Therefore, the threshold values for this case study will be adjusted to 100 for K_f and 5 for K_r. The decision to trip the circuit will be made when both relays detect the fault. The total time required for fault isolation is the sum of the fault detection time by the relays, which is 20 ms, the communication time between relays, also 20 ms, and the time required for the circuit breaker to disconnect the circuit, also 20 ms.

If communication between the relays is lost, the relay will trip 60 ms after the fault is detected, as depicted in the relays flowchart in Fig. 5. This delay serves to distinguish between fault and normal conditions, such as load switching at the reverse relay, as shown in table 10. The total time required for fault isolation in this case will be the sum of the fault detection time by the relays (20 ms), the relay delay time (60 ms), and the time required for the circuit breaker to disconnect the circuit (20 ms).

For comparison purposes, the author in [27] choose to use db 8 as mother wavelet function, testing the current signal. The author suggested using d2 and d3 to be used to identify the HIF from other events. The main disadvantages of this method are the large time required to detect the fault and the numerous system-dependent adjustments (Ad2, Ad3, D HIF, timer, and X). This brief analysis of the work presented in [27] demonstrates the effectiveness of the suggested algorithm, whose required time is less than that presented in [27] and also with simple adjustment.

C. RESULTS OF ONLINE CALCULATIONS

The online calculations concerned current measurements used to detect various faults, centralized communication to identify the OM and relay settings, and decentralized communication between relays in the same feeder to improve the protection system's accuracy and speed. Consequently, the results of this section will be presented as a calculation of the required time to detect and isolate the faulted feeder for various scenarios in order to verify the algorithm's validity and speed. Calculating the detection and isolation time is possible by observing the flowcharts of the relays depicted in Fig. 5.

1) SCENARIO 1: FAULT DETECTION AND ISOLATION WITH THE COMMUNICATION EXISTENCE BETWEEN RELAYS

In this scenario, the time required to protect the system from overload, short circuit, and HIF will be calculated based on existence of communication, relay measurements, and the predefined OM. This case represents the system's default case. For the purpose of calculating isolation time, the flowchart of the relays depicted in Fig. 5 will be monitored as shown in Fig. 10. It is important to note that the time required to execute the relay program's steps depends on the relay processor. Therefore, this time is negligible and will have no effect on the protection time. The graph illustrates that the total time required for fault isolation is 60 ms if the circuit breaker successfully disconnected and 100 ms if the breaker failed to disconnect and the backup relay and circuit breaker disconnected the circuit.

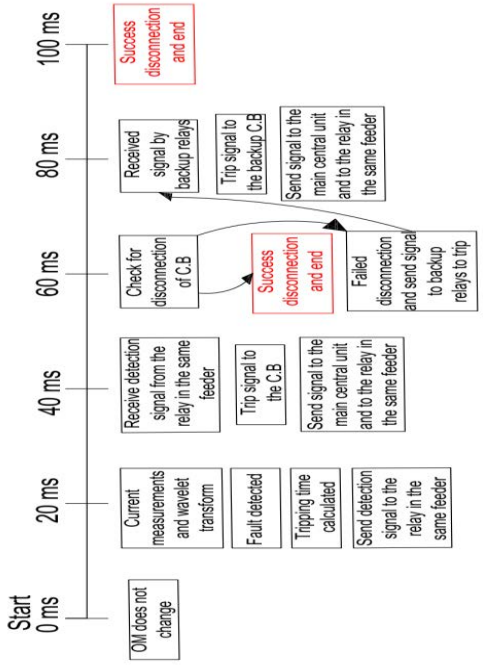

FIGURE 10. Time required for overload, short circuit, and HIF clearance in the case of communication and measurements existence.

2) SCENARIO 2: HIF DETECTION AND ISOLATION, BUT THE RELAY IN THE SAME FEEDER FAILED TO CONFIRM FAULT DETECTION

This case demonstrates the operation of the relay to protect the system from HIF in the event that the relay in the same feeder failed to confirm fault detection due to a loss of communication link or malfunctioning measurement devices. In this instance, the relay will operate independently. To identify fault, the relay will require 20 ms to apply wavelet transform to the current wave. Then, the relay will activate at the predetermined trip time of 60 ms. The delay of 60 ms is necessary to distinguish between HIF and other events and prevent false tripping, as the decision will be made by a single relay. So, the total time for sending the trip signal from the relay to the circuit breaker is 80 ms, and the total clearance time after the circuit breaker is disconnected will be 100 ms, as shown in Fig. 11. This time will be increased by 40 ms if the circuit breaker fails to disconnect the circuit and the backup circuit breaker is used instead.

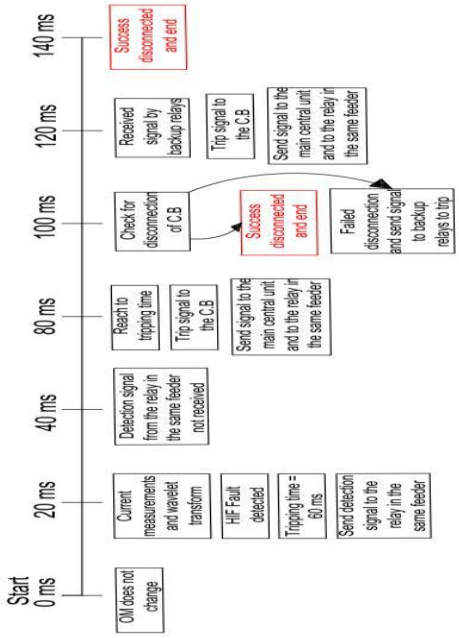

FIGURE 11. Time required for HIF clearance in the case of fault detection not confirmed from the relay in the same feeder.

3) SCENARIO 3: OVERLOAD AND SHORT CIRCUIT FAULTS DETECTION AND ISOLATION, BUT THE RELAY IN THE SAME FEEDER FAILED TO CONFIRM FAULT DETECTION

This case demonstrates the operation of a relay to protect the system from overload and short circuit faults if the relay in the same feeder failed to confirm fault detection due to a loss of communication link or malfunctioning measuring devices. In this instance, the relay will function as a conventional digital relay. It will take 20 ms for the relay to

measure current and identify a fault. The relay will then determine and activate the trip time based on the

characteristic curve. Therefore, the required time depends on the fault current and the relay's curve. Notably, the relay curve was chosen based on the results of an optimization problem solved using GA. Consequently, this curve will achieve proper coordination and fast fault isolation in comparison to conventional methods. In addition, this can be assumed to be an emergency condition for the system, and the system will return to its normal state once the fault has been detected and confirmed by both relays in the same feeder. In this instance, the total isolation time will be 40 + x ms, where x is the tripping time calculated from the characteristic curve and 40 ms are the fault detection time by the relay and isolation time by the circuit breaker. This time will be increased by 40 ms if the circuit breaker fails to disconnect the circuit and the backup circuit breaker is used instead.

VI. CONCLUSION

This paper proposes a combination of centralized and decentralized communication to overcome all protection issues associated with the connection of DGs to the existing power grid and to detect HIF with high speed and precision. The proposed algorithm employs two directional relays with communication capabilities in each feeder. When a relay's status changes from connected to disconnected or vice versa, the centralized communication between the central unit and the relays in the system is carried out. This communication is used to identify the OM, the islanding operation, and to activate the relay settings that achieve proper relay coordination. In the case of HIF, decentralized communication is used to increase the accuracy and speed of the protection system. When any relay detects a fault, the decentralized communication is initiated. All relay variables, including pickup current, TMS, PSM, and curve type, are factored into the optimization problem as part of the coordination between relays, which is performed using GA. ETAP is used to perform system simulation, load flow analysis, and short circuit calculations, while MATLAB is used to execute the GA routine. HIF detection is carried out utilizing Wavelet transform, Symlet 8, d2 to extract the signal's features. The HIF is determined by adding the squares of all d2 values over a cycle. The proposed method is applied to the IEC benchmark microgrid system, and the results demonstrate the algorithm's superiority over existing techniques in terms of speed and accuracy.

REFERENCES

[1] J. A. Martinez and J. Martin-Arnedo, "Impact of distributed generation on distribution protection and power quality," in *Proc. IEEE Power Energy Soc. Gen. Meeting*, Jul. 2009, pp. 1–6, doi: 10.1109/PES.2009.5275777.

[2] A. Alipour and M. Pacis, "Optimal coordination of directional overcurrent relays (DOCR) in a ring distribution network with distributed generation (DG) using genetic algorithm," in *Proc. IEEE Region 10 Conf. (TENCON)*, Nov. 2016, pp. 3109–3112, doi: 10.1109/TENCON.2016.7848621.

[3] P. P. Bedekar and S. R. Bhide, "Optimum coordination of overcurrent relay timing using continuous genetic algorithm," *Expert Syst. Appl.*, vol. 38, pp. 11286–11292, Sep. 2011.

[4] J. M. Ghogare and V. N. Bapat, "Field based case studies on optimal coordination of overcurrent relays using genetic algorithm," in *Proc. IEEE Int. Conf. Electr., Comput. Commun. Technol. (ICECCT)*, Mar. 2015, pp. 1–7, doi: 10.1109/ICECCT.2015.7225940.

[5] R. Madhumitha, P. Sharma, D. Mewara, O. V. G. Swathika, and S. Hemamalini, "Optimum coordination of overcurrent relays using dual simplex and genetic algorithms," in *Proc. Int. Conf. Comput. Intell. Commun. Netw. (CICN)*, 2015, pp. 1544–1547, doi: 10.1109/CICN.2015.342.

[6] D. S. Alkaran, M. R. Vatani, M. J. Sanjari, G. B. Gharehpetian, and M. S. Naderi, "Optimal overcurrent relay coordination in interconnected networks by using fuzzy-based GA method," *IEEE Trans. Smart Grid*, vol. 9, no. 4, pp. 3091–3101, Jul. 2018, doi: 10.1109/TSG.2016.2626393.

[7] S. V. Chakor and T. N. Date, "Optimum coordination of directional overcurrent relay in presence of distributed generation using genetic algorithm," in *Proc. 10th Int. Conf. Intell. Syst. Control (ISCO)*, Jan. 2016, pp. 1–5, doi: 10.1109/ISCO.2016.7727078.

[8] R. A. Swief, A. Y. Abdelaziz, and A. Nagy, "Optimail strategy for over current relay coordination using genetic algorithm," in *Proc. Int. Conf. Eng. Technol. (ICET)*, Apr. 2014, pp. 1–5, doi: 10.1109/ICENGTECHNOL.2014.7016786.

[9] D. K. Singh and S. Gupta, "Use of genetic algorithms (GA) for optimal coordination of directional over current relays," in *Proc. Students Conf. Eng. Syst.*, Mar. 2012, pp. 1–5, doi: 10.1109/SCES.2012.6199087.

[10] M. N. Alam, "Overcurrent protection of AC microgrids using mixed characteristic curves of relays," *Comput. Electr. Eng.*, vol. 74, pp. 74–88, Mar. 2019.

[11] S. M. Saad, N. El-Naily, and F. A. Mohamed, "A new constraint considering maximum PSM of industrial over-current relays to enhance the performance of the optimization techniques for microgrid protection schemes," *Sustain. Cities Soc.*, vol. 44, pp. 445–457, Jan. 2019.

[12] N. El-Naily, S. M. Saad, T. Hussein, and F. A. Mohamed, "A novel constraint and non-standard characteristics for optimal over-current relays coordination to enhance microgrid protection scheme," *IET Gener., Transmiss. Distrib.*, vol. 13, no. 6, pp. 780–793, Mar. 2019.

[13] S. D. Saldarriaga-Zuluaga, J. López-Lezama, and J. M. Muñoz-Galeano, "Optimal coordination of overcurrent relays in microgrids considering a non-standard characteristic," *Energies*, vol. 13, no. 4, p. 922, 2020.

[14] S. D. Saldarriaga-Zuluaga, J. M. López-Lezama, and N. Muñoz-Galeano, "Adaptive protection coordination scheme in microgrids using directional over-current relays with non-standard characteristics," *Heliyon*, vol. 7, no. 4, Apr. 2021, Art. no. e06665.

[15] A. S. Aljankawey, W. G. Morsi, L. Chang, and C. P. Diduch, "Passive method-based islanding detection of renewable-based distributed generation: The issues," in *Proc. IEEE Electr. Power Energy Conf.*, Aug. 2010, pp. 1–8, doi: 10.1109/EPEC.2010.5697253.

[16] X. Zhu, C. Du, G. Shen, M. Chen, and D. Xu, "Analysis of the non-detection zone with passive islanding detection methods for current control DG system," in *Proc. 24th Annu. IEEE Appl. Power Electron. Conf. Expo.*, Feb. 2009, pp. 358–363, doi: 10.1109/APEC.2009.4802682.

[17] P. Mahat, Z. Chen, and B. Bak-Jensen, "A hybrid islanding detection technique using average rate of voltage change and real power shift," *IEEE Trans. Power Del.*, vol. 24, no. 2, pp. 764–771, Apr. 2009, doi: 10.1109/TPWRD.2009.2013376.

[18] A. Samui and S. R. Samantaray, "Assessment of ROCPAD relay for islanding detection in distributed generation," *IEEE Trans. Smart Grid*, vol. 2, no. 2, pp. 391–398, Jun. 2011, doi: 10.1109/TSG.2011.2125804.

[19] M. R. Alam, K. M. Muttaqi, and A. Bouzerdoum, "An approach for assessing the effectiveness of multiple-feature-based SVM method for islanding detection of distributed generation," *IEEE Trans. Ind. Appl.*, vol. 50, no. 4, pp. 2844–2852, Jul./Aug. 2014, doi: 10.1109/TIA.2014.2300135.

[20] C. Abbey, Y. Brissette, and P. Venne, "An autoground system for anti-islanding protection of distributed generation," *IEEE Trans. Power Syst.*, vol. 29, no. 2, pp. 873–880, Mar. 2014, doi: 10.1109/TPWRS.2013.2284670.

[21] Y. Fayyad and A. Osman, "Neuro-wavelet based islanding detection technique," in *Proc. IEEE Electr. Power Energy Conf.*, Aug. 2010, pp. 1–6, doi: 10.1109/EPEC.2010.5697180.

[22] G. Hernandez-Gonzalez and R. Iravani, "Current injection for active islanding detection of electronically-interfaced distributed resources," *IEEE Trans. Power Del.*, vol. 21, no. 3, pp. 1698–1705, Jul. 2006, doi: 10.1109/TPWRD.2006.876980.

[23] S. Wang and P. Dehghanian, "On the use of artificial intelligence for high impedance fault detection and electrical safety," *IEEE Trans. Ind. Appl.*, vol. 56, no. 6, pp. 7208–7216, Nov./Dec. 2020, doi: 10.1109/TIA.2020.3017698.

[24] M. S. Tonelli-Neto, J. G. M. S. Decanini, A. D. P. Lotufo, and C. R. Minussi, "Fuzzy based methodologies comparison for high-impedance fault diagnosis in radial distribution feeders," *IET Gener., Transmiss. Distrib.*, vol. 11, no. 6, pp. 1557–1565, Apr. 2017.
[25] B. Wang, J. Geng, and X. Dong, "High-impedance fault detection based on nonlinear voltage–current characteristic profile identification," *IEEE Trans. Smart Grid*, vol. 9, no. 4, pp. 3783–3791, Jul. 2018, doi: 10.1109/TSG.2016.2642988.
[26] M. R. Haghifam, A. R. Sedighi, and O. P. Malik, "Development of a fuzzy inference system based on genetic algorithm for high impedance fault detection," *IEE Proc.-Gener., Transmiss. Distrib.*, vol. 153, no. 3, pp. 359–367, May 2006.
[27] G. D. A. Ferreira and T. M. L. Assis, "A novel high impedance arcing fault detection based on the discrete wavelet transform for smart distribution grids," in *Proc. IEEE PES Innov. Smart Grid Technol. Conf.-Latin Amer. (ISGT Latin Amer.)*, Sep. 2019, pp. 1–6, doi: 10.1109/ISGT-LA.2019.8895264.
[28] K. Sekar, N. K. Mohanty, and A. K. Sahoo, "High impedance fault detection using wavelet transform," in *Proc. Technol. Smart-City Energy Secur. Power (ICSESP)*, Mar. 2018, pp. 1–6, doi: 10.1109/ICSESP.2018.8376740.
[29] K. Moloi, J. A. Jordaan, and Y. Hamam, "High impedance fault detection technique based on discrete wavelet transform and support vector machine in power distribution networks," in *Proc. IEEE AFRICON*, Sep. 2017, pp. 9–14, doi: 10.1109/AFRCON.2017.8095447.
[30] A. Oudalov and A. Fidigatti, "Adaptive network protection in microgrids," *Int. J. Distrib. Energy Resour.*, vol. 5, no. 3, pp. 201–226, 2009.
[31] T. S. Ustun, C. Ozansoy, and A. Zayegh, "Modeling of a centralized microgrid protection system and distributed energy resources according to IEC 61850-7-420," *IEEE Trans. Power Syst.*, vol. 27, no. 3, pp. 1560–1567, Aug. 2012, doi: 10.1109/TPWRS.2012.2185072.
[32] M. A. Zamani, A. Yazdani, and T. S. Sidhu, "A communication-assisted protection strategy for inverter-based medium-voltage microgrids," *IEEE Trans. Smart Grid*, vol. 3, no. 4, pp. 2088–2099, Dec. 2012, doi: 10.1109/TSG.2012.2211045.
[33] H. Lin, J. M. Guerrero, C. Jia, Z.-H. Tan, J. C. Vasquez, and C. Liu, "Adaptive overcurrent protection for microgrids in extensive distribution systems," in *Proc. 42nd Annu. Conf. IEEE Ind. Electron. Soc.*, Oct. 2016, pp. 4042–4047, doi: 10.1109/IECON.2016.7793091.
[34] H. Lin, K. Sun, Z. Tan, C. Liu, J. M. Guerrero, and J. C. Vasquez, "Adaptive protection combined with machine learning for microgrids," *IET Gener., Transmiss. Distrib.*, vol. 13, no. 6, pp. 770–779, Mar. 2019.
[35] S. M. E. Ghadiri and K. Mazlumi, "Adaptive protection scheme for microgrids based on SOM clustering technique," *Appl. Soft Comput.*, vol. 88, Mar. 2020, Art. no. 106062.
[36] A. E. C. Momesso, W. M. S. Bernardes, and E. N. Asada, "Adaptive directional overcurrent protection considering stability constraint," *Electr. Power Syst. Res.*, vol. 181, Apr. 2020, Art. no. 106190.
[37] M. S. Javadi, A. E. Nezhad, A. Anvari-Moghaddam, and J. M. Guerrero, "Optimal overcurrent relay coordination in presence of inverter-based wind farms and electrical energy storage devices," in *Proc. IEEE Int. Conf. Environ. Elect. Eng. IEEE Ind. Commercial Power Syst. Eur.*, Jun. 2018, pp. 1–5, doi: 10.1109/EEEIC.2018.8494605.
[38] A. A. de Sotomayor, D. D. Giustina, G. Massa, A. Dedè, F. Ramos, and A. Barbato, "IEC 61850-based adaptive protection system for the MV distribution smart grid," *Sustain. Energy, Grids Netw.*, vol. 15, pp. 26–33, Sep. 2018.
[39] P. H. A. Barra, D. V. Coury, and R. A. S. Fernandes, "A survey on adaptive protection of microgrids and distribution systems with distributed generators," *Renew. Sustain. Energy Rev.*, vol. 118, Feb. 2020, Art. no. 109524.
[40] S. Beheshtaein, R. Cuzner, M. Savaghebi, and J. M. Guerrero, "Review on microgrids protection," *IET Gener., Transmiss. Distrib.*, vol. 13, no. 6, pp. 743–759, 2019.
[41] B. Mahamedi and J. E. Fletcher, "Trends in the protection of inverter-based microgrids," *IET Gener. Transm. Distrib.*, vol. 13, pp. 4511–4522, Oct. 2019.
[42] N. Hussain, M. Nasir, J. C. Vasquez, and J. M. Guerrero, "Recent developments and challenges on AC microgrids fault detection and protection systems—A review," *Energies*, vol. 13, no. 9, p. 2149, May 2020.
[43] B. Patnaik, M. Mishra, R. C. Bansal, and R. K. Jena, "AC microgrid protection—A review: Current and future prospective," *Appl. Energy*, vol. 271, Aug. 2020, Art. no. 115210.
[44] S. Kar, S. R. Samantaray, and M. D. Zadeh, "Data-mining model based intelligent differential microgrid protection scheme," *IEEE Syst. J.*, vol. 11, no. 2, pp. 1161–1169, Jun. 2017, doi: 10.1109/JSYST.2014.2380432.
[45] A. A. Memon and K. Kauhaniemi, "An adaptive protection for radial AC microgrid using IEC 61850 communication standard: Algorithm proposal using offline simulations," *Energies*, vol. 13, no. 20, p. 5316, Oct. 2020.
[46] S. Gautam and S. M. Brahma, "Detection of high impedance fault in power distribution systems using mathematical morphology," *IEEE Trans. Power Syst.*, vol. 28, no. 2, pp. 1226–1234, May 2013, doi: 10.1109/TPWRS.2012.2215630.
[47] M. F. Akorede and H. Hizam, "Wavelet transforms: Practical applications in power systems," *J. Electr. Eng. Technol.*, vol. 4, no. 2, pp. 168–174, Jun. 2009.

ALAA HMAM EL-HAMRAWY was born in Baltim, Egypt, in 1988. He received the B.Sc. and M.Sc. degrees in electrical engineering from Alexandria University, Alexandria, Egypt, in 2012 and 2018, respectively. He is currently pursuing the Ph.D. degree in electrical engineering. He is currently a Teaching Assistant with Alexandria University. His research interests include power system protection, distributed generation, and smart grids.

AHMED ABDEL MORDI EBRAHIEM was born in Egypt, in 1970. He received the B.S. and M.S. degrees from Alexandria University, Egypt, in 1993 and 1998, respectively, and the Ph.D. degree from Heriot Watt University, Edinburgh, Scotland, U.K., in 2004. He is currently a Full Lecturer with the Electrical Department, Faculty of Engineering, Alexandria University. His research interests include power quality, renewable energy, and power systems.

ASHRAF IBRAHIM MEGAHED (Member, IEEE) was born in Alexandria, Egypt, in 1969. He received the B.Sc. and M.Sc. degrees in electrical engineering from Alexandria University, Alexandria, in 1991 and 1994, respectively, and the Ph.D. degree from the University of Calgary, Calgary, AB, Canada, in 1998. He is currently a Professor with Alexandria University. His research interests include digital protection, application of neural networks, and wavelet transform in protection.